Daytime Evolution of Relative Humidity at the Boundary Layer Top

M. EK AND L. MAHRT

Oceanic and Atmospheric Sciences, Oregon State University, Corvallis, Oregon

(Manuscript received 29 November 1993, in final form 9 April 1994)

ABSTRACT

Data from the Hydrological and Atmospheric Pilot Experiment-Modélisation du Bilan Hydrique (HAPEX-MOBILHY) field program and results from a one-dimensional model of the soil and atmospheric boundary layer are analyzed to study the daytime evolution of the relative humidity at the boundary layer top. This evolution is thought to control the development of boundary layer clouds. This study examines the dependence of boundary layer relative humidity on soil moisture, large-scale vertical motion, and the moisture content and temperature stratification above the boundary layer. The response of the boundary layer relative humidity to external forcing involves competing mechanisms and the net effect on relative humidity is difficult to predict without complete analysis of the relative humidity tendency equation.

As one example, drier soil leads to smaller boundary layer specific humidity but also leads to cooler temperatures at the boundary layer top due to greater boundary layer growth. When the latter effect dominates, the relative humidity at the boundary layer top is greater over drier soil. In contrast, drier soil leads to lower relative humidity at the boundary layer top when the air above the boundary layer is strongly stratified or quite dry. These and other nonlinear interactions are posed in terms of a detailed analysis of the budget equation for boundary layer top relative humidity.

1. Introduction

The daytime evolution of the boundary layer moisture field and potential for boundary layer cloud development depends, in part, on soil moisture, large-scale vertical motion, and the "dryness" of the air above the growing boundary layer. These dependencies can sometimes contribute to unexpected changes of the boundary layer relative humidity through nonlinear interactions shown in Fig. 1.

Consider the following two examples. Strong low-level subsidence inversions normally suppress the development of boundary layer clouds. However, with low sun angle and moist soil conditions, boundary layer relative humidity may increase with a strong low-level inversion and lead to the development of boundary layer stratus. As a second example, dry soil conditions are normally expected to reduce the probability of boundary layer cloud development. However, with less surface evaporation or transpiration, greater surface heating leads to deeper boundary layer growth, which can sometimes lead to boundary layer cloud development in spite of weaker surface evaporation (see Otterman et al. 1990; Rabin et al. 1990; Lanicci et al. 1987; Colby 1984). The prediction of one outcome versus the other in these examples depends on external conditions and complex boundary layer interactions.

To study the above boundary layer interactions, the daytime evolution of the boundary layer relative humidity field using data from the Hydrological and Atmospheric Pilot Experiment-Modélisation du Bilan Hydrique (HAPEX-MOBILHY) (André et al. 1988) will be examined. The data is interpreted using a simple one-dimensional model that couples the atmospheric boundary layer, vegetation, and soil. The ensuing study will focus on the evolution of relative humidity near the top of the growing daytime boundary layer.

2. Boundary layer relative humidity

To understand the physics of the examples described in the introduction, the tendency equation for relative humidity (RH) is analyzed:

$$\frac{\partial(\mathrm{RH})}{\partial t} = \frac{\partial}{\partial t}\left(\frac{q}{q_s}\right) = \frac{1}{q_s}\frac{\partial q}{\partial t} - \frac{\mathrm{RH}}{q_s}\frac{\partial q_s}{\partial t} = \frac{1}{q_s}\frac{\partial q}{\partial t} - \frac{\mathrm{RH}}{q_s}\frac{dq_s}{dT}\frac{\partial T}{\partial t}, \quad (1)$$

where q is the specific humidity, q_s is saturation specific humidity, dq_s/dT is the slope of the saturation specific humidity–temperature curve, and T is temperature.

Corresponding author address: Michael Ek, Oceanic and Atmospheric Sciences, Oregon State University, Corvallis, OR 97331-5503.

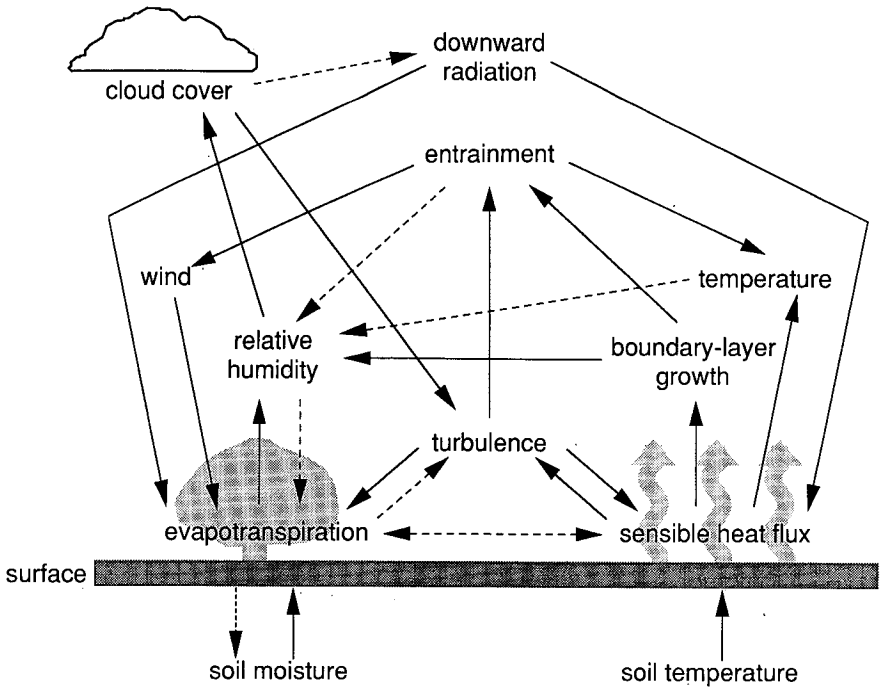

FIG. 1. Suspected important interactions between the surface and boundary layer for conditions of daytime surface heating. Solid arrows indicate the direction of feedbacks that are normally positive (leading to an increase of the recipient variable). Dashed arrows indicate negative feedbacks. Two consecutive negative feedbacks make a positive one. Note the many positive and negative feedback loops that may lead to increased or decreased relative humidity and cloud cover.

With well-mixed conditions, the relative humidity reaches a maximum near the boundary layer top that will be the reference level for the following developments. The relative humidity tendency combines the separate influences of changes in moisture and changes in temperature, the first and second terms on the right-hand side of (1), respectively, where these tendencies are influenced by different boundary layer and land surface processes. This development is continued to explicitly account for these different processes.

Assuming a well-mixed boundary layer, the temperature tendency is expressed as

$$\frac{\partial T}{\partial t} = \frac{\partial}{\partial t}\left[\theta\left(\frac{p}{p_s}\right)^{R/c_p}\right],$$

which can be eventually written as

$$\frac{\partial T}{\partial t} = \left(\frac{p}{p_s}\right)^{R/c_p}\frac{\partial \theta}{\partial t} + \frac{T}{p}\frac{R}{c_p}\frac{\partial p}{\partial t}, \qquad (2)$$

where θ is potential temperature, p is pressure, p_s is surface pressure, R is the gas constant, c_p is specific heat of air, and the equation of state and the definition of potential temperature have been used. Using the hydrostatic approximation and neglecting the local change of pressure at a fixed height, the pressure tendency can be written as

$$\frac{\partial p}{\partial t} = \frac{\partial p}{\partial z}\frac{\partial h}{\partial t} = -\rho g\frac{\partial h}{\partial t} = -\frac{pg}{RT}\frac{\partial h}{\partial t}, \qquad (3)$$

where h is the boundary layer depth, z is height, ρ is air density, and g is gravity. Substituting (3) into (2) gives

$$\frac{\partial T}{\partial t} = \left(\frac{p}{p_s}\right)^{R/c_p}\frac{\partial \theta}{\partial t} - \frac{g}{c_p}\frac{\partial h}{\partial t}. \qquad (4)$$

Substituting (4) into (1) then gives

$$\frac{\partial(\mathrm{RH})}{\partial t} = \frac{1}{q_s}\frac{\partial q}{\partial t} - \frac{\mathrm{RH}}{q_s}\frac{dq_s}{dT}\left[\left(\frac{p}{p_s}\right)^{R/c_p}\frac{\partial \theta}{\partial t} - \frac{g}{c_p}\frac{\partial h}{\partial t}\right]. \qquad (5)$$

To avoid modeling the vertical structure of specific humidity, well-mixed conditions in specific humidity as well as potential temperature are assumed. The equations for the boundary layer moisture and thermodynamic budgets from Tennekes (1973) are

$$\frac{\partial q}{\partial t} = -\frac{1}{h}([w'q']_h - [w'q']_s) \qquad (6a)$$

$$\frac{\partial \theta}{\partial t} = -\frac{1}{h}([w'\theta'])_h - [w'\theta']_s), \qquad (6b)$$

where $[w'q']$ and $[w'\theta']$ are the moisture and heat fluxes, respectively, and the subscripts s and h refer to

the surface and the level just below the boundary layer top, respectively. Substituting (6a) and (6b) into (5) gives

$$\frac{\partial(\mathrm{RH})}{\partial t} = \frac{1}{hq_s}([w'q']_s - [w'q']_h) - \frac{\mathrm{RH}}{q_s}\frac{dq_s}{dT} \times \left\{\left(\frac{p}{p_s}\right)^{R/c_p}\frac{1}{h}([w'\theta']_s - [w'\theta']_h) - \frac{g}{c_p}\frac{\partial h}{\partial t}\right\}. \quad (7)$$

To simplify the "bookkeeping," *variable* coefficients are defined as

$$C_\theta \equiv -\frac{[w'\theta']_h}{[w'\theta']_s} \quad (8a)$$

$$C_q \equiv \frac{[w'q']_h}{[w'q']_s}. \quad (8b)$$

Under many conditions, $C_\theta \approx C$, where $C = [w'\theta'_v]_h/[w'\theta'_v]_s$ and is often found in the literature. In daytime boundary layers, the value of C_θ is typically thought to range between 0.2 and 0.5 (Betts et al. 1990; Tennekes and Driedonks 1981; Carson 1973) but can be much larger in cases of significant shear generation of turbulence and weak surface heating (Nicholls and LeMone 1980). The value of C_q is more variable, exceeding unity in the drying boundary layer (Mahrt 1991; Betts et al. 1990; Steyn 1990) and often becoming 0.5 or less in the moistening boundary layer (Grant 1986; Nicholls and Reading 1979; and others).

Using (8a) and (8b), the relative humidity tendency equation (7) becomes

$$\frac{\partial(\mathrm{RH})}{\partial t} = \underset{(1)}{c_0[w'q']_s} - \underset{(2)}{c_0C_q[w'q']_s} - \underset{(3)}{c_1[w'\theta']_s(1 + C_\theta)} + \underset{(4)}{c_2 h\frac{\partial h}{\partial t}}, \quad (9)$$

where

$$c_0 = \frac{1}{hq_s}$$

$$c_1 = c_0\mathrm{RH}\frac{dq_s}{dT}\left(\frac{p}{p_s}\right)^{R/c_p}$$

$$c_2 = c_0\mathrm{RH}\frac{dq_s}{dT}\frac{g}{c_p}.$$

The four terms on the right-hand side of (9) are

1) increasing relative humidity due to surface evapotranspiration;

2) decreasing relative humidity due to entrainment of dry air from above the boundary layer ($C_q > 0$), or less commonly, increasing relative humidity due to entrainment of moister air from above the boundary layer ($C_q < 0$);

3) decreasing relative humidity due to surface sensible heat flux and entrainment of warmer air at the boundary layer top (boundary layer warming); and

4) increasing relative humidity due to increasing boundary layer depth where for a given potential temperature, the temperature at the boundary layer top decreases with boundary layer growth.

The importance of these different effects in different atmospheric situations is now estimated.

a. Boundary layer warming and growth

In this section, the influence of moisture changes on the evolution of relative humidity is neglected, in which case the relative humidity at the boundary layer top changes due to adiabatic cooling from boundary layer growth and due to the turbulent heat flux. The importance of boundary layer heating with respect to the boundary layer growth can be expressed as the ratio of term 3 to term 4:

$$\left(\frac{p}{p_s}\right)^{R/c_p}[w'\theta']_s(1 + C_\theta)\left[\frac{g}{c_p}h\frac{\partial h}{\partial t}\right]^{-1}. \quad (10)$$

The boundary layer warming can be neglected if it is small compared to $(g/c_p)(\partial h/\partial t) \sim [1°\mathrm{C}\ (100\ \mathrm{m})^{-1}](\partial h/\partial t)$. This condition is met during the late morning rapid growth period, but otherwise the heating term cannot be categorically neglected.

For the simplified case where the mean vertical motion and horizontal advection are small, the turbulence is generated primarily by buoyancy effects, and where the time rate of change of the inversion strength is small compared to the boundary layer heating rate, the boundary layer depth tendency may be approximated as (Tennekes 1973; Betts 1973)

$$\frac{\partial h}{\partial t} = \frac{[w'\theta']_s(1 + C_\theta)}{h\gamma_\theta}, \quad (11)$$

where γ_θ is the vertical gradient of potential temperature above the boundary layer. Then the time rate of change of relative humidity at the boundary layer top is

$$\frac{\partial(\mathrm{RH})}{\partial t} = -\frac{\mathrm{RH}}{hq_s}\frac{dq_s}{dT}(1 + C_\theta) \times \left[\left(\frac{p}{p_s}\right)^{R/c_p} - \frac{1}{\gamma_\theta}\frac{g}{c_p}\right][w'\theta']_s. \quad (12a)$$

The ratio of the effects of boundary layer growth to the boundary layer warming from (10) assumes the approximate form

$$\frac{g}{c_p}\frac{1}{\gamma_\theta}\left(\frac{p}{p_s}\right)^{-R/c_p}. \quad (12b)$$

If the stratification of potential temperature is small compared to $g/c_p \sim 1°C\ (100\ m)^{-1}$, the influence of the surface heat flux on the boundary layer growth effect will exceed the direct effect of boundary layer warming. This condition is easily met in those late morning periods where the boundary layer has consumed the nocturnal surface inversion and grows rapidly through the residual layer remaining from the mixed layer of the previous day. This condition is approximated in many atmospheric situations, including that of the standard atmosphere. However, in general, the boundary layer warming term must be included.

If the air aloft is quite dry, (12a) will overestimate the increase of relative humidity because of neglect of entrainment drying of the boundary layer, the subject of the next subsection.

b. Dry-air entrainment

For cases where boundary layer warming can be neglected compared to the boundary layer growth, only the additional influence of changes of moisture need be considered. The relative humidity at the boundary layer top increases with time unless the boundary layer dries at a rate that exceeds the boundary layer growth term. This can occur only with rapid entrainment of dry air. To study the case of boundary layer drying, the dry-air entrainment is approximated as

$$-[w'q']_h = \Delta q \frac{\partial h}{\partial t}, \tag{13}$$

where Δq is the change of specific humidity across the boundary layer top, which is normally negative, and the mean vertical motion is zero [analogous to Tennekes (1973), his Eq. (1); see also Ball (1960), Kraus and Turner (1967), and Lilly (1968)]. Then the ratio of the magnitude of the effects of surface evaporation and boundary layer growth to the effect of entrainment drying is

$$\frac{1}{C_q} - \mathrm{RH}\left(\frac{dq_s}{dT}\right)\frac{g}{c_p}\frac{h}{\Delta q}. \tag{14}$$

Note that (14) is independent of the boundary layer growth rate since the dry-air entrainment [term 2 in (9)] and boundary layer growth [term 4 in (9)] are both linearly proportional to the growth rate.

Since C_q is likely to be large when Δq is large and vice versa, (14) must be evaluated on a case by case basis. The analyses in sections 3 and 4 suggest that the relative humidity at the boundary layer top will normally increase during the day in which case (14) exceeds unity. This is not surprising since boundary layer clouds are more likely to develop as the boundary layer deepens. However, the above analysis provides a framework for estimating how fast the relative humidity increases with time prior to cloud development and whether cloud formation will be possible. Additionally, the daytime evolution of the real atmospheric boundary layer is significantly influenced by soil moisture and the large-scale vertical motion, the subject of the next two sections.

c. Influence of soil moisture and surface evaporation

Greater soil moisture leads to boundary layer moistening, which acts to increase the relative humidity, but also leads to weaker surface heating and weaker boundary layer growth, which may in turn lead to smaller values of relative humidity at the boundary layer top. As a result of these opposing influences, the net effect of soil moisture changes on relative humidity at the boundary layer top and the potential for boundary layer cloud development cannot be simply predicted.

To study the influence of soil moisture, note that the boundary layer growth due to surface heating is inversely related to the surface moisture flux through the surface energy balance

$$\rho c_p[w'\theta']_s = R_n - G - \rho L_v[w'q']_s, \tag{15}$$

where R_n is the net radiation, L_v is the latent heat of evaporation, and G is the soil heat flux.

Substituting (15) into the relative humidity tendency equation (9) and using the simplified expression for the convectively generated mixing depth (11), yields

$$\frac{\partial(\mathrm{RH})}{\partial t} = \frac{1}{hq_s}\left\{[w'q']_s(1 - C_q) + \left(\frac{A^*}{\gamma_\theta} - B^*\right) \times \left(\frac{R_n - G}{\rho L_v} - [w'q']_s\right)\right\}, \tag{16}$$

where

$$A^* \equiv \mathrm{RH}\frac{dq_s}{dT}\frac{L_v}{c_p}(1 + C_\theta)\frac{g}{c_p}$$

$$B^* \equiv \mathrm{RH}\frac{dq_s}{dT}\frac{L_v}{c_p}(1 + C_\theta)\left(\frac{p}{p_s}\right)^{R/c_p}.$$

Collecting the direct influence of the surface evaporation on the boundary layer moisture with the indirect effect of the surface moisture flux on reduction of boundary layer growth (16) becomes

$$\frac{\partial(\mathrm{RH})}{\partial t} = \frac{1}{hq_s}\left\{[w'q']_s\left(1 - \frac{A^*}{\gamma_\theta} + B^*\right) - [w'q']_h + \left(\frac{A^*}{\gamma_\theta} - B^*\right)\left(\frac{R_n - G}{\rho L_v}\right)\right\}. \tag{17}$$

The entrainment term $[w'q']_h$ normally acts to decrease relative humidity.

Surface evaporation acts to increase relative humidity at the boundary layer top if

$$\frac{\gamma_\theta(1 + B^*)}{A^*} > 1. \tag{18}$$

This situation occurs with strong stratification in which case the primary role of surface evaporation is to moisten the boundary layer. Then greater soil moisture and evaporation increase the relative humidity at the boundary layer top and thus increase the probability of boundary layer cloud development, as in Hammer (1970) and Barnston and Schikedanz (1984). This interaction is sometimes used to construct a feedback mechanism in extended drought or desertification arguments; that is, that drier soil leads to lower relative humidity at the boundary layer top (Oglesby and Erickson 1989; Namias 1988; Trenberth et al. 1988; and others).

On the other hand, if the stratification above the boundary layer is weak, Eq. (18) <1, then the relative humidity tendency is strongly influenced by the boundary layer growth term. As a result, the main influence of surface evaporation on relative humidity is to reduce the boundary layer growth term and thus reduce relative humidity at the boundary layer top. Therefore with weak stratification, *drier* soil increases the probability of boundary layer cloud development, as in Otterman et al. (1990), Rabin et al. (1990), and others.

The above arguments are based on a number of simplifications leading to (18). Drought scenarios are further complicated by the interdependence of $[w'q']_h$, γ_θ, A^* and B^*, and the necessity to include cloud feedback mechanisms; both are beyond the scope of this discussion. Even in the above oversimplified example, the role of soil moisture is complex indicating that construction of desertification scenarios can be misleading.

d. Large-scale vertical motion

To estimate the influence of the mean vertical motion w_h on the relative humidity tendency, (9) is differentiated with respect to the mean vertical motion and again we neglect the direct influence of surface heating on the relative humidity to obtain

$$\frac{\partial}{\partial w_h}\frac{\partial(\mathrm{RH})}{\partial t} = -\left\{\frac{[w'q']_s(1-C_q)}{q_s h^2}\right\}\frac{\partial h}{\partial w_h} + \frac{g}{c_p}\frac{\mathrm{RH}}{q_s}\frac{dq_s}{dT}, \quad (19)$$

where it is noted that $(\partial/\partial w_h)(\partial h/\partial t) = 1$. Even though the entrainment rate is normally time dependent, the complex physics of this equation can be qualitatively examined in terms of scale values for the case of a time-independent entrainment rate w_e and mean vertical motion

$$h = (w_e + w_h)t. \quad (20)$$

Then $\partial h/\partial w_h = t$ and (19) becomes

$$\frac{\partial}{\partial w_h}\frac{\partial(\mathrm{RH})}{\partial t} = -\left\{\frac{[w'q'](1-C_q)}{q_s h^2}\right\}t + \frac{g}{c_p}\frac{\mathrm{RH}}{q_s}\frac{dq_s}{dT}. \quad (21)$$

This equation represents the change of relative humidity tendency with respect to changes of mean vertical motion. For the case of mean subsidence ($w_h < 0$), negative values of terms on the right-hand side of (21) indicate greater positive tendency of relative humidity and therefore greater relative humidity. The change of relative humidity ΔRH over time period T^* due to enhanced subsidence Δw_h (<0) would be

$$\Delta\mathrm{RH} = -\Delta w_h T^* \times\left\{\frac{T^*[w'q']_s(1-C_q)}{q_s h^2} - \frac{g}{c_p}\frac{\mathrm{RH}}{q_s}\frac{dq_s}{dT}\right\}. \quad (22)$$

The first term represents the increase of relative humidity due to "trapping" of evaporated surface moisture in a thinner boundary layer. The second term represents the slower rate of relative humidity decrease at the boundary layer top due to slower boundary layer growth. The relative importance of the first term is accumulative and thus increases with time. Therefore, the initial influence of subsidence is to cause decreasing values of the relative humidity at the boundary layer top as a result of slower boundary layer growth compared to the case without subsidence.

However, after the timescale

$$\tau = \frac{g}{c_p}\mathrm{RH}\frac{dq_s}{dT}h^2\{[w'q']_s(1-C_q)\}^{-1}, \quad (23)$$

the net influence of the subsidence is to increase the relative humidity through trapping of boundary layer moisture. Then subsidence and reduced boundary layer growth may increase the probability of boundary layer cloud development (Mahrt and Pierce 1980). With large surface moisture flux and weaker entrainment of dry air (C_q small), the stage at which the subsidence acts to increase the relative humidity begins sooner. In winter with a thin boundary layer depth, the timescale from (23) will be small and the main influence of subsidence will be to increase the relative humidity through trapping of moisture.

On the other hand, if this time is comparable to, or large compared to the period of mixed-layer development, then the main influence of subsidence is the decrease of boundary-layer depth leading to smaller relative humidity at the boundary layer top compared to the case of no subsidence.

e. Small boundary layer growth

When boundary layer growth is small, typically in the early morning or later afternoon over land or in the quasi-steady marine boundary layer, the boundary layer growth term in the relative humidity tendency equation can be ignored. Then the relative humidity tendency is determined by surface evaporation, boundary layer warming and dry air entrainment.

To estimate the relative importance of increased relative humidity at the boundary layer top due to surface

evaporation compared to decreased relative humidity due to boundary layer warming and dry entrainment, involves the ratio

$$[w'q']_s\left\{\mathrm{RH}\,\frac{dq_s}{dT}\left(\frac{p}{p_s}\right)^{R/c_p}[w'\theta']_s \times (1 + C_\theta) + [w'q']_s C_q\right\}^{-1}, \quad (24)$$

which can be rewritten as

$$L_v[w'q']_s\left\{\mathrm{RH}\,\frac{dq_s}{dT}\frac{L_v}{c_p}\left(\frac{p}{p_s}\right)^{R/c_p}c_p[w'\theta']_s \times (1 + C_\theta) + L_v[w'q']_s C_q\right\}^{-1} \quad (25)$$

and reduces to

$$\frac{1}{\beta B^* + C_q}, \quad (26)$$

where β is the (surface) Bowen ratio and B^* is defined in section 2c. When the ratio (26) is greater than unity the relative humidity will increase with time. For example, over land in the early morning or afternoon when boundary layer growth and entrainment are weak, a low Bowen ratio leads to increasing relative humidity at the boundary layer top.

The above analysis provides a framework for studying the evolution of the boundary layer top relative humidity. The examples cited above have not exhausted the important possibilities. Other important examples include the slowly varying marine boundary layer. In this study, the terms in (9) are now evaluated by examining observations taken during HAPEX-MOBILHY.

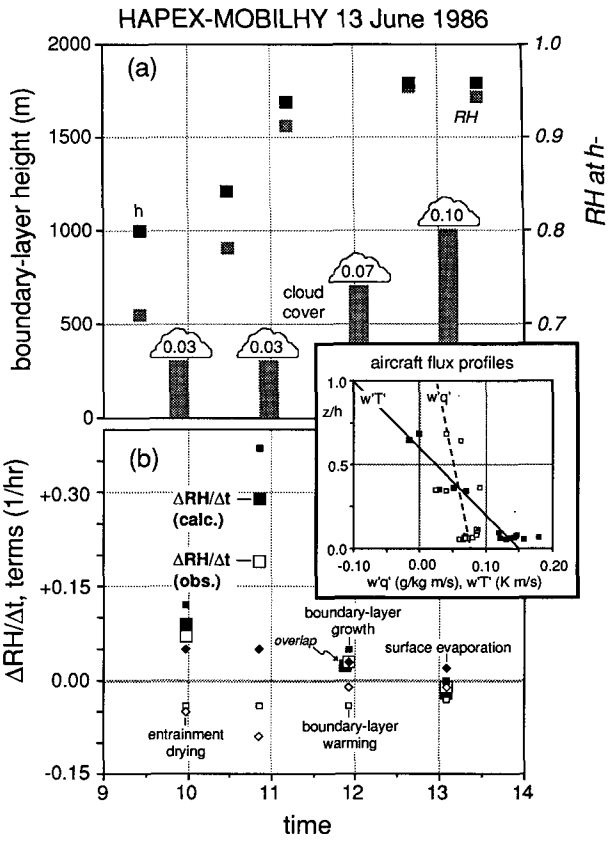

FIG. 2. (a) Observed boundary layer depth, relative humidity at boundary layer top, and fractional cloud cover; (inset) heat and moisture aircraft flux profiles; and (b) observed relative humidity tendency at the boundary layer top; and tendency terms and computed relative humidity tendency evaluated from Eq. (9) from aircraft data for 13 June 1986 in HAPEX-MOBILHY.

3. HAPEX-MOBILHY data analysis

a. Aircraft data

To evaluate the terms in the relative humidity tendency equation (9) aircraft observations made at multiple levels in the boundary layer on a fair weather day during HAPEX-MOBILHY (André et al. 1988) are examined. During this field program considerable attention was devoted to aircraft moisture measurements (Eloranta et al. 1988). On 13 June 1986 atmospheric conditions were the most homogeneous across the experimental domain compared to other flight days, and boundary layer cloud fractions averaged 10% or less. This aircraft flight was from 0853 to 1354 UTC (solar time) and included the morning rapid boundary layer growth.

Boundary layer depth is estimated using relative humidity profiles from the five aircraft slant soundings (Fig. 2a). Relative humidity combines the influences of decreasing moisture and increasing temperature with height to provide a sharper delineation of the boundary layer top (Mahrt 1976). Fractional cloud cover is determined using an upward-looking solar radiometer (Ek and Mahrt 1991) and is the average cloud cover for the horizontal aircraft flight legs between soundings. Flux measurements from the aircraft horizontal flight legs were computed using a high-pass filter with a 5-km wavelength (Mahrt 1991), with mid- and upper-level flights after the rapid growth of the boundary layer. Surface flux values are taken as an average of the low-level flights nearest to the sounding time.

During slower boundary layer growth after 1100, flux profiles (Fig. 2, inset) are used to determine ratios of the boundary layer top fluxes to the surface fluxes [the values of C_θ and C_q defined in (8)]. A linear fit to the average flux values at each of the three aircraft flight levels is extrapolated to the boundary layer top, yielding values of $C_\theta = 0.67$ and $C_q = 0.33$. Here C_θ is larger than the more theoretical free convection value of 0.2 because of the observed wind shear on this day, about 5 m s^{-1} per 100 m at the boundary layer top.

TABLE 1. Values of C_θ and C_q, tendency terms and relative humidity tendency from Eq. (9), and observed relative humidity tendency for 13 June 1986 in HAPEX-MOBILHY. Tendencies are extrapolated to hourly values for easier interpretation.

Time (UTC)	C_θ	C_q	Surface evaporation	Dry-air entrainment	BL warming	BL growth	RH tendency (calc)	RH tendency (obs)
0958	0.67	0.82	0.06	−0.05	−0.04	0.12	+0.09	+0.07
1051	0.67	2.05	0.05	−0.09	−0.04	0.37	+0.29	+0.19
1156	0.67	0.33	0.03	−0.01	−0.04	0.05	+0.03	+0.03
1304	0.67	0.33	0.02	−0.01	−0.03	0.00	−0.02	−0.01

The value of C_q is expected to be larger during the rapid growth of the boundary layer when entrainment is strong. Aircraft flux measurements from the middle and upper boundary layer are unavailable during the rapid growth of the boundary layer before 1100, so the value of C_q is estimated from aircraft sounding moisture profiles using a graphical integration method. This method follows Stull [1988, his Eq. (11.2.2c)] applied to moisture flux expressed in finite difference form, so that

$$C_q = \Delta h \frac{\Delta q}{\Delta t} \frac{1}{[w'q']_s}, \qquad (27)$$

where Δh is the change in the boundary layer depth between the two soundings, Δq is the average time change in the specific humidity over the layer between the two boundary layer tops, and Δt is the time between aircraft soundings. The large-scale subsidence and advection of moisture appear to be small compared to the boundary layer growth rate during this time since specific humidity is constant with time above the growing boundary layer. The value of C_q exceeds unity during rapid growth of the boundary layer, implying boundary layer drying; C_q is less than unity after 1100, implying vertical convergence of moisture flux and daytime boundary layer moistening. Temperature advection does seem to be important during this period so that soundings could not be used to estimate C_θ. Therefore, C_θ is assigned the same value as estimated from aircraft fluxes later in the day. Here C_θ is constrained by the turbulence energy budget and is expected to be less variable than C_q.

Centered time differencing is used to estimate tendency terms from (9) for four different times (Table 1, Figure 2b).[1] Atmospheric conditions on 13 June show rapid growth of the boundary layer until 1100 (Fig. 2a). The boundary layer growth term dominates the relative humidity tendency during this period (Fig. 2b, Table 1), with the observed relative humidity increasing from about 0.70 to more than 0.95. The small fractional cloud cover was observed to increase during the rapid boundary layer growth, similar to Johnson's (1977) findings that cumulus convection over Florida first developed during the late morning rapid growth period. Additionally, even though the observed average relative humidity was less than 1.0, clouds formed because of spatial variations of relative humidity (Betts 1983; Wilde et al. 1985; Ek and Mahrt 1991).

Relative to the other terms, the boundary layer growth term dominates only during the period of rapid boundary layer growth before 1100, with the rest of the relative humidity tendency terms in (9) becoming important in the early afternoon after boundary layer growth diminishes. Note that the relative humidity tendency is overpredicted during the rapid growth of the boundary layer (Table 1), perhaps because of errors in the estimates of the effects of entrainment during the period of rapid boundary layer growth. In the early afternoon the relative humidity becomes approximately time independent with a value of about 0.95.

Evaluation of (26) for the case of negligible boundary layer growth is valid in the early afternoon near the end of the flight (section 2e). During this period the value of (26) is less than unity predicting that the relative humidity will decrease (as observed) because of the dominance of dry air entrainment and boundary layer warming over surface evaporation.

b. *Simple models*

Although the radiosonde dataset does not provide flux values, it does allow partial evaluation of the relative humidity tendency from (9). The aircraft case

[1] Increasing or decreasing the values of C or C_q by a factor of 2 changes the relative humidity tendency by about 0.05 h^{-1} or less. Typical errors in the surface flux measurements on the order of 20% yield differences in the relative humidity tendency equation on the order of 0.01 h^{-1}. Errors in the flux measurements are particularly large in the upper part of the boundary layer where the scale of the transporting eddies is large. The errors are estimated as $\sigma_{flux} n^{-1/2}$, where σ_{flux} is the standard deviation of the flux and n is the number of independent flux measurements, yielding estimates of 0.005 m s^{-1} °C for the heat flux (30% of the mean flux value) and 0.019 m s^{-1} g kg^{-1} for the moisture flux (almost 40% of the mean flux value) for this day. Estimating boundary layer depth subjectively from relative humidity profiles, errors on the order of 100 m h^{-1} in the boundary layer depth tendency might be expected, which gives a difference in the relative humidity tendency of about 0.05 h^{-1}. These potential errors in estimating tendency terms are less important when the boundary layer growth term dominates the relative humidity tendency.

study of 13 June in HAPEX-MOBILHY shows that the relative humidity tendency in the morning is dominated by the boundary layer growth term, a term that can be estimated from radiosonde data. For the 13 June aircraft data, the observed relative humidity tendency is modestly correlated with the boundary layer growth term (oversized squares, Fig. 3a).

To supplement the above aircraft analysis, boundary layer radiosonde data for 10 fair weather days during HAPEX-MOBILHY 1986 are examined (Brutsaert and Parlange 1992). Radiosondes were launched from the forest clearing at the central site of Lubbon at approximately 2-h intervals (0600–1800). The boundary layer top is determined by visual inspection of sounding profiles of relative humidity. Although the instantaneous radiosonde observations are less reliable estimates of the mean structure of the boundary layer compared to aircraft slant soundings, the radiosonde dataset provides a larger sample size. We restrict our analysis to the cases where boundary layer growth exceeds 100 m h^{-1}. At smaller growth rates the uncertainties in the radiosonde dataset make estimates of the boundary layer growth less reliable.

From the radiosonde dataset, the boundary layer growth term in (9) is computed and modest correlation with the observed relative humidity tendency at the boundary layer top is found (Fig. 3a). The regression equation using the boundary layer growth term alone is

$$\frac{\Delta \mathrm{RH}}{\Delta t} = a_0 + a_1 \mathrm{BLG}, \qquad (28)$$

where $a_0 = -0.036$ and $a_1 = 0.36$, and BLG is the boundary layer growth term from (9) in finite-difference form. To generalize (28), (13) is used to construct a rough estimate of the boundary layer top entrainment flux and the entrainment drying term. The observed relative humidity tendency is linearly regressed with the boundary layer growth and entrainment drying terms to obtain

$$\frac{\Delta \mathrm{RH}}{\Delta t} = b_0 + b_1(\mathrm{BLG} + \mathrm{DAE}), \qquad (29)$$

where $b_0 = -0.029$ and $b_1 = 0.55$, and DAE is the dry-air entrainment term using (13) in finite-difference form. The correlation between the observed relative humidity tendency and that predicted from (29) increases when this entrainment drying term is included (Fig. 3b). The generality of (28) and (29) is not known and additional datasets are required before (29) can be considered a useful prediction of boundary layer cloud formation.

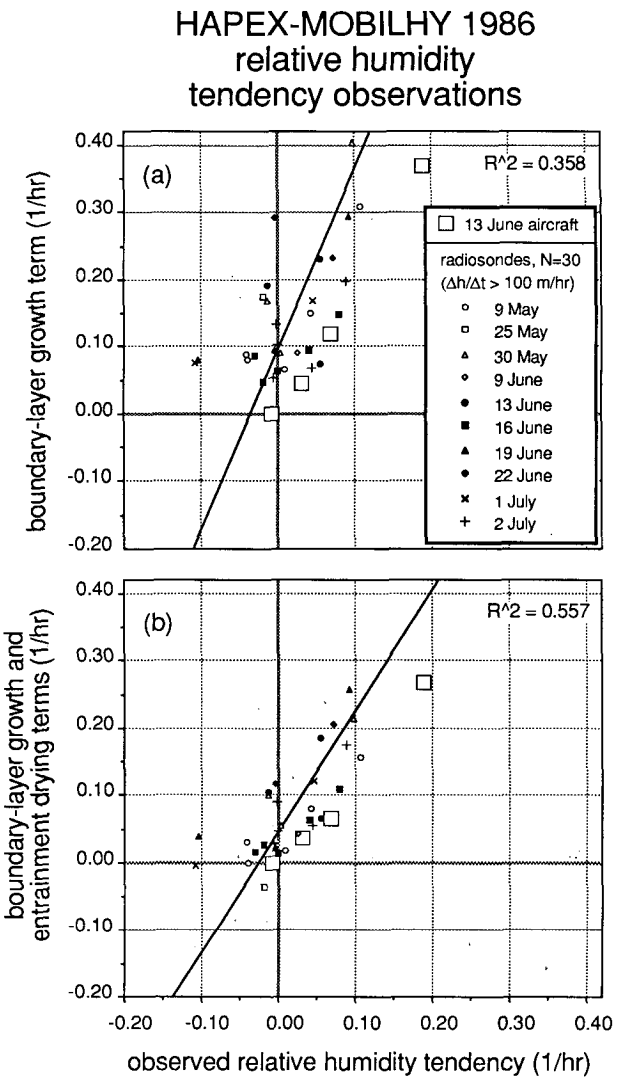

FIG. 3. Observed relative humidity tendency and terms in the relative humidity tendency equation evaluated from radiosonde data for 10 days in HAPEX-MOBILHY 1986 (13 June aircraft data in oversized symbols), (a) observed relative humidity tendency versus the boundary layer growth term alone, (b) observed relative humidity tendency versus the sum of the boundary layer growth and entrainment drying terms.

4. Boundary layer model simulations

All the terms in (9) are now evaluated from sensitivity tests utilizing the Oregon State University one-dimensional coupled atmospheric–plant–soil model that was developed to simulate the interactions of the atmospheric boundary layer, vegetation, and soil. The atmospheric boundary layer model (Troen and Mahrt 1986; Holtslag et al. 1990; Holtslag and Boville 1993) is coupled with an active two-layer soil model and a simple vegetated surface (Pan and Mahrt 1987) using the Penman–Monteith formulation. For the sensitivity tests, data from the pine forest region in southwest France taken during HAPEX-MOBILHY is used (André et al. 1988; Noilhan and Planton 1989), with a momentum roughness length of 1.0 m, and a smaller

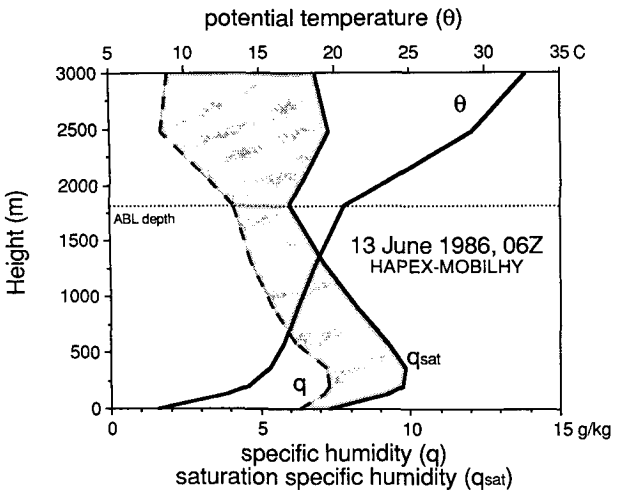

FIG. 4. Radiosonde data profiles at 0600 UTC 13 June 1986 in HAPEX-MOBILHY showing saturation specific humidity q_{sat}, specific humidity q, and potential temperature θ used in model initiation, and the approximate observed maximum afternoon boundary layer depth (dotted line).

TABLE 2. Summary of initial conditions for model sensitivity tests.

13 June	
• Prototype	geostrophic wind, northeast at 10 m s^{-1} subsidence, 2 cm s^{-1} at 5 km average volumetric soil mositure content, $\Theta \approx 0.15$
• Dry aloft	RH $\approx$ 0.80 near the surface, decreasing to 0.20 at 3 km
• Moist aloft	RH $\approx$ 0.80 near the surface, increasing to 0.95 at 3 km
• Dry soil	Θ = 0.07, model vegetation wilting point
• Moist soil	Θ = 0.435, model soil moisture saturation
22 June	
◦ Prototype	geostrophic wind, southwest at 12 m s^{-1} subsidence, 3.5 cm s^{-1} at 5 km average volumetric soil moisture content, $\Theta \approx 0.12$
• Dry soil	Θ = 0.07, model vegetation wilting point
• Moist soil	Θ = 0.435, model soil moisture saturation

value of 10^{-2} m for the roughness length for heat following Mahrt and Ek (1993). Geostrophic winds and vertical motion values are taken from the mesoscale analysis described in Jacquemin and Noilhan (1990). Mean vertical motion is specified to increase linearly with height from zero at the surface and is fitted to an "observed"-layer averaged value centered at 2 km, and a 12-h-averaged value centered at 1200 UTC (solar time). Geostrophic wind is assumed constant with time.

We first make a prototype simulation for the 13 June case, initiating the model using the 0600 radiosonde data (Fig. 4). While the data does not allow formal verification, the model results for 13 June compare favorably with the observed conditions (Fig. 5a). Modeled relative humidity near the boundary layer top is about 0.10 larger than that observed by the aircraft and radiosonde data earlier in the observing period, but agrees more closely with data later in the day. For the prototype model simulation, apparently advection was not important and the subsidence value was reasonably well estimated (Ek and Mahrt 1991). A summary of initial conditions for model sensitivity tests is shown in Table 2.

a. Evolution stages

Four stages of moisture development occur on 13 June, which also occurred to various degrees on other days during HAPEX-MOBILHY. We briefly discuss these stages for the prototype simulation in terms of the relative humidity tendency terms (Fig. 5b) and the evolution of relative humidity near the boundary layer top (Fig. 6). On 13 June, the observed boundary layer was relatively moist and grew to about 1800 m by midday.

Stage 1: Early-morning moistening (0600–0700) — Surface fluxes are weak with weak turbulent moisture

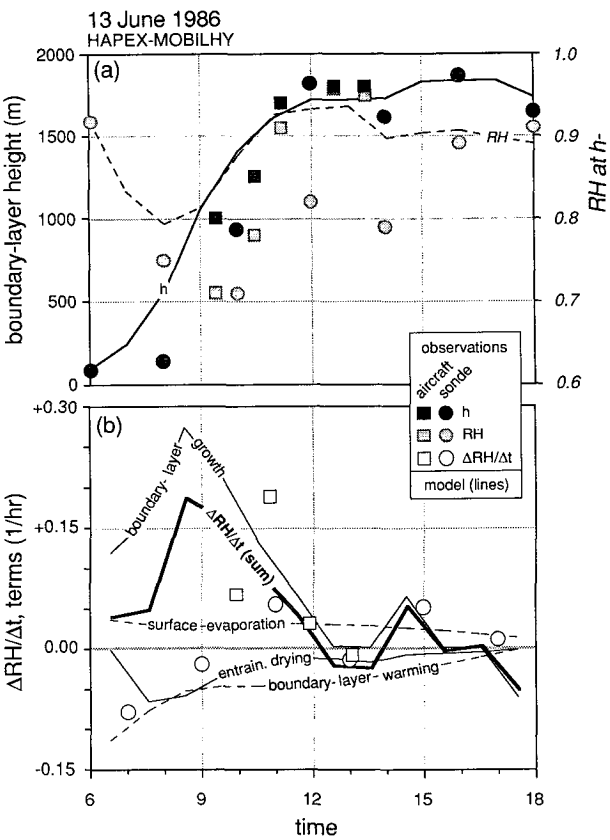

FIG. 5. Daytime evolution of (a) the boundary layer depth and relative humidity at the boundary layer top, and (b) the four relative humidity tendency terms and total relative humidity tendency from Eq. (9) for the prototype model simulation (solid lines), and aircraft and radiosonde observations (symbols defined in inset) for 13 June 1986 in HAPEX-MOBILHY.

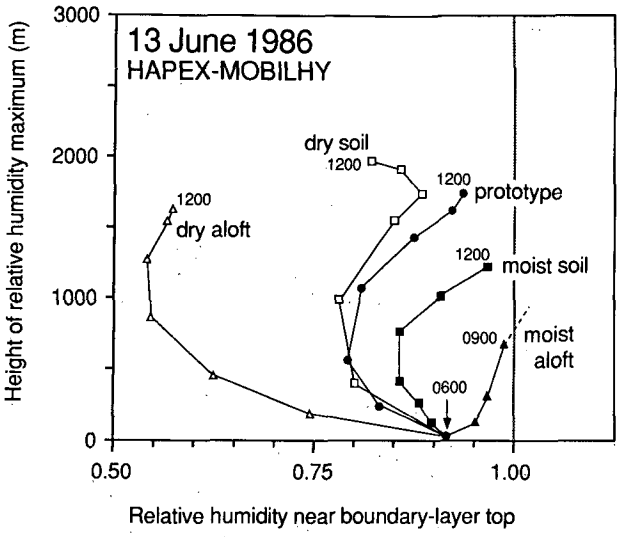

FIG. 6. Daytime evolution of relative humidity near the boundary layer top for the different model sensitivity tests described in section 4 for 13 June 1986 in HAPEX-MOBILHY.

flux convergence and moistening of the shallow boundary layer. Due to surface heating, however, at the top of the boundary layer temperature increases sufficiently for relative humidity to decrease.

Stage 2: Mid- to late-morning rapid growth (0700–1100)—Boundary layer growth becomes rapid with stronger vertical moisture flux divergence induced by dry air entrainment. This flux divergence decreases the boundary layer specific humidity; however, the relative humidity near the boundary layer top increases due to the large boundary layer growth term in (9).

Stage 3: Early afternoon (1100–1500)—After the rapid growth stage, boundary layer specific humidity increases slightly due to vertical convergence of the turbulent moisture flux. This flux convergence is associated with reduced boundary layer growth and reduced dry-air entrainment and increasing surface evapotranspiration. However, the relative humidity at the boundary layer top decreases slowly with time due to the slight excess of the boundary layer warming term over surface evaporation term.

Stage 4: Mid- to late-afternoon diminishing surface fluxes (1500–1800)—Surface fluxes decrease and the change in relative humidity at the boundary layer top is small.

Aspects of the first two stages are documented in previous studies. Coulman (1978) shows moisture flux convergence and boundary layer moistening in the early morning when boundary layer growth is weak, followed by stronger boundary layer growth with moisture flux divergence and boundary layer drying (see Mahrt 1991). Segal et al. (1991) show similar results where the low-level moisture increases in early morning in the shallow boundary layer, then decreases rapidly as the morning surface inversion is eroded by a growing boundary layer. This same rapid moisture decrease also occurred at the forest tower near the central site (Fig. 7) and at some of the surface observing network (12 surface stations) for 13 June 1986 in HAPEX-MOBILHY. However, after the initial moisture decrease, there is a steady increase throughout the rest of the day at the forest tower site corresponding to a moistening boundary layer ($C_q < 1$). Compare this to 22 June 1986 in HAPEX-MOBILHY (discussed further below) where low-level moisture increases in the early morning shallow boundary layer and then decreases due to the growing boundary layer. This decrease continues throughout the day of 22 June, which is identified as a boundary layer drying day with $C_q > 1$.

The model simulations are terminated at noon since the relative humidity at the boundary layer top exceeds 1.0 in the afternoon for several of the simulations in which case a cloud model would be required. As expected, drier (moister) air above the boundary layer leads to more (less) dry-air entrainment and lower (greater) relative humidity at the boundary layer top (Fig. 6).

b. Influence of soil moisture

The influence of soil moisture on relative humidity varies dramatically according to initial atmospheric conditions and the prescribed mean subsidence. The effect of soil moisture on relative humidity tendency described by (18) involves the opposing influences of boundary layer moistening and reduced boundary layer growth due to surface evaporation. For 13 June, (18)

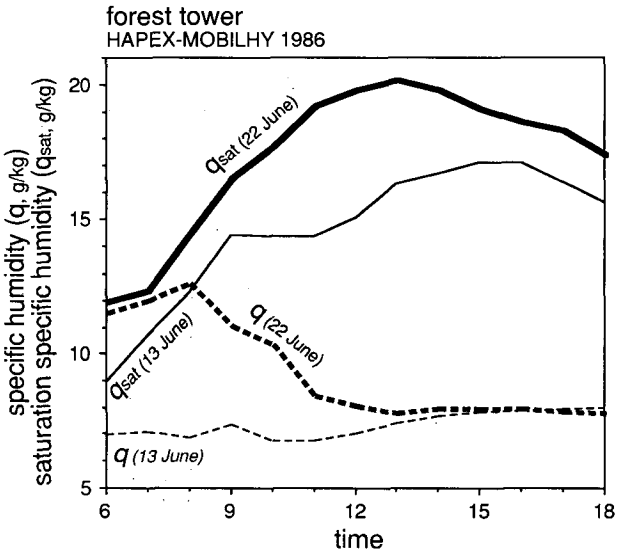

FIG. 7. Time series of specific humidity and saturation specific humidity at the forest tower site in HAPEX-MOBILHY for 13 and 22 June 1986.

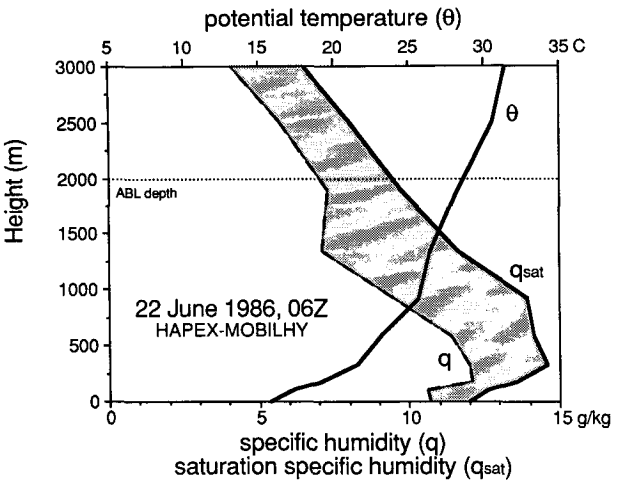

FIG. 8. As in Fig. 4 except for 22 June 1986 in HAPEX-MOBILHY.

is greater than unity during most of the day because of significant temperature stratification above the boundary layer. This suggests that the main influence of surface evaporation for this day is to increase the relative humidity at the boundary layer top. When the soil is specified to be dry (Fig. 6, Table 2), greater surface heating leads to more rapid boundary layer growth. The increase of relative humidity due to greater boundary layer growth is opposed by the effects of stronger surface heating, dry air entrainment, and decreased surface evaporation. As a result, the decrease of soil moisture exerts little net effect on the relative humidity at the boundary layer top before noon (Fig. 6). However, by noon when boundary layer growth diminishes, relative humidity at the boundary layer top decreases with time due to stronger surface heating compared to the prototype case. For the case of very moist soil, boundary layer growth diminishes by noon due to less surface heating. Then the greater surface evaporation leads to greater relative humidity compared to the prototype case.

To further examine the effect of temperature stratification and moisture aloft on the relative humidity tendency, sensitivity tests are made for 22 June 1986 in HAPEX-MOBILHY, again initiating the model using 0600 radiosonde data (Fig. 8, Table 2). On 22 June, the observed boundary layer was relatively dry but with greater moisture aloft. Temperature stratification was weaker, which allowed for deeper boundary layer growth compared to 13 June. The greater spatial inhomogeneity on 22 June precludes analysis of the relative humidity tendency in the same manner as the more spatially homogeneous case on 13 June.

Repeating the same soil moisture sensitivity tests above for 22 June indicates that the soil moisture exerts the opposite influence on the relative humidity at the boundary layer top compared to 13 June. With dry soil and weaker temperature stratification, the boundary layer grows rapidly. The influence of dry-air entrainment is only modest because the air aloft is relatively moist (Fig. 9). As a result, the relative humidity at the boundary layer top is greater for drier soil compared to the prototype case! For moist soil conditions, the influence of greater surface evaporation on relative humidity is largely offset by slower boundary layer growth, so the relative humidity at the boundary layer top is smaller for moist soil compared to the drier soil case.

From a more general point of view, drier soil may or may not decrease relative humidity and cloud development at the boundary layer top, depending on temperature stratification and moisture aloft. Therefore, the role of soil moisture cannot be simply predicted as assumed in some climate feedback arguments.

All three model simulations for the 22 June case overpredict the observed relative humidity by 0.05–0.10, possibly due to the exclusion of modest dry air advection at upper levels after the model initialization at 0600. Note that this overprediction cannot be ameliorated by adjusting soil moisture.

As possible implications of the above sensitivity tests, consider typical High Plains conditions or regions of synoptic-scale subsidence where the air above the boundary layer is quite dry (Palmén and Newton 1969). Then drier soil and resulting large boundary layer growth is more likely to decrease the relative humidity at the top of the boundary layer. In contrast, consider typical conditions further east with moist southerly flow aloft. Then drier soil conditions and greater boundary layer growth can lead to larger relative humidity at the boundary layer top.

Plants provide a conduit for deep soil moisture to the atmosphere. The effect of moistening due to transpi-

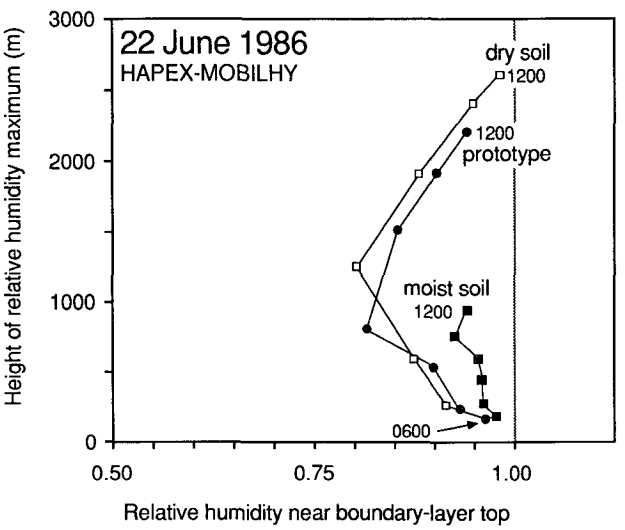

FIG. 9. As in Fig. 6 except for 22 June 1986 in HAPEX-MOBILHY.

ration is offset by weaker surface heating and resulting weaker boundary layer growth. Then the relative humidity for a fully vegetated surface (simulation not shown) is similar to values for the bare soil case for a range of initial conditions. As with all sensitivity tests, the above results do not indicate general rules, but provide only examples for a specific set of initial conditions and parameter values.

5. Conclusions

Aircraft observations from a case study fair weather day in HAPEX-MOBILHY have been analyzed to evaluate terms in the tendency equation for relative humidity at the boundary layer top (9). These findings were extended to include 10 days of radiosonde data, and simulations with a one-dimensional numerical model for two contrasting days in HAPEX-MOBILHY. The analyses indicate that the adiabatic decrease of the boundary layer top temperature during the morning rapid boundary layer growth exerts the strongest influence on the relative humidity tendency. That is, as the boundary layer top grows to lower pressure, the temperature and saturation vapor pressure decrease for a given potential temperature. Of course the potential temperature and specific humidity of the boundary layer are both changing, so that the net change of relative humidity at the boundary layer top is the difference between several effects as represented by (9). Based on analysis of HAPEX-MOBILHY data, a simple version of the relative humidity tendency equation (29) is constructed. However, (29) requires comparison with additional datasets before it can be assessed as a predictive tool.

If the air aloft is characterized by weak stratification and is not too dry, the relative humidity at the boundary layer top and probability of cloud initiation might increase more rapidly over dry surfaces than over wet surfaces. In this case, the more rapid growth over dry surfaces is the main influence on relative humidity at the boundary layer top. This case appears to explain increased convection and cloud development over surfaces of large sensible heat flux compared to surfaces with enhanced moisture flux (Otterman et al. 1990; Rabin et al. 1990; and others). However, if the air above the boundary layer is characterized by significant stratification, the boundary layer relative humidity is generally greater over moist surfaces where boundary layer growth is weaker (Hammer 1970; Barnston and Schikedanz 1984). This case includes the drought feedback mechanism of dry spring soil conditions where reduced soil moisture reduces the probability of precipitation thus intensifying drought conditions (Oglesby and Erickson 1989; Namias 1988; Trenberth et al. 1988; and others); this scenario is more likely to occur with dry air aloft in which case the more rapid growth of the boundary layer over dry surfaces leads to entrainment drying of the boundary layer. Previously proposed drought scenarios are generally valid only for a specific parameter regime. Modeling drought conditions as well as forecasting boundary layer cloud development requires adequate representation of several different boundary layer interactions controlling the relative humidity field.

Acknowledgments. The detailed comments by reviewers Alan Betts and Doug Lilly are greatly appreciated. This material is based upon work supported by the Phillips Laboratory under Contract F19628-91-K-0002, and the NOAA Climate and Global Change Program under Award NA36GP0369. The National Center for Atmospheric Research is acknowledged for the use of the King Air research aircraft in HAPEX-MOBILHY.

REFERENCES

André, J.-C., and coauthors, 1988: HAPEX-MOBILHY: First results from the special observing period. *Ann. Geophys. Ser. B,* **6,** 477–492.

Ball, F. K., 1960: Control of inversion height by surface heating. *Quart. J. Roy. Meteor. Soc.,* **86,** 483–494.

Barnston, A. G., and P. T. Schikedanz, 1984: The effect of irrigation on warm season precipitation in the southern Great Plains. *J. Climate Appl. Meteor.,* **23,** 865–888.

Betts, A. K., 1973: Non-precipitating cumulus convection and its parameterization. *Quart. J. Roy. Meteor. Soc.,* **99,** 178–196.

——, 1983: Thermodynamics of mixed stratocumulus layers: Saturation point budgets. *J. Atmos. Sci.,* **40,** 2655–2670.

——, R. L. Desjardins, J. I. MacPherson, and R. D. Kelly, 1990: Boundary-layer heat and moisture budgets from FIFE. *Bound.-Layer Meteor.,* **50,** 109–137.

Brutsaert, W., and M. B. Parlange, 1992: The unstable surface layer above forest: Regional evaporation and heat flux. *Water Resour. Res.,* **28,** 3129–3134.

Carson, D. J., 1973: The development of a dry inversion-capped convectively unstable boundary layer. *Quart. J. Roy. Meteor. Soc.,* **99,** 450–467.

Colby, F. P., 1984: Convective inhibition as a prediction of convection during AVE-SESAME II. *Mon. Wea. Rev.,* **112,** 2239–2252.

Coulman, C. E., 1978: Boundary-layer evolution and nocturnal inversion dispersal—Part 1: *Bound.-Layer Meteor.,* **14,** 471–491.

Ek, M., and L. Mahrt, 1991: A model for boundary-layer cloud cover. *Ann. Geophys.,* **9,** 716–724.

Eloranta, D., R. Stull, and E. Ebert, 1988: Test of a calibration device for airborne Lyman-alpha hygrometers. *J. Atmos. Oceanic Technol.,* **6,** 129–139.

Grant, A. L. M., 1986: Observations of boundary layer turbulence made during the 1981 KONTUR experiment. *Quart. J. Roy. Meteor. Soc.,* **112,** 825–841.

Hammer, R. M., 1970: Cloud development and distribution around Khartoum. *Weather,* **25,** 411–414.

Holtslag, A. A. M., and B. Boville, 1993: Local versus nonlocal boundary-layer diffusion in a global climate model. *J. Climate,* **6,** 1825–1842.

——, E. I. F. de Bruijn, and H.-L. Pan, 1990: A high-resolution air mass transformation model for short-range weather forecasting. *Mon. Wea. Rev.,* **118,** 1561–1575.

Jacquemin, B., and J. Noilhan, 1990: Sensitivity study and validation of a land surface parameterization using the HAPEX-MOBILHY data set. *Bound.-Layer Meteor.,* **52,** 93–134.

Johnson, R. H., 1977: Effects of cumulus convection on the structure and growth of the mixed layer over south Florida. *Mon. Wea. Rev.,* **105,** 713–724.

Kraus, E. B., and J. S. Turner, 1967: A one-dimensional model of the seasonal thermocline. II. The general theory and its consequences. *Tellus,* **19,** 98–105.

Lanicci, J. M., T. N. Carlson, and T. T. Warner, 1987: Sensitivity of the Great Plains environment to soil moisture distribution. *Mon. Wea. Rev.,* **115,** 2660–2673.

Lilly, D. K., 1968: Models of cloud-topped mixed layers under a strong inversion. *Quart. J. Roy. Meteor. Soc.,* **94,** 292–309.

Mahrt, L., 1976: Mixed layer moisture structure. *Mon. Wea. Rev.,* **104,** 1403–1407.

——, 1991: Boundary-layer moisture regimes. *Quart. J. Roy. Meteor. Soc.,* **117,** 151–176.

——, and D. A. Pierce, 1980: Relationship of moist convection to boundary layer properties: Application to a semi arid region. *Mon. Wea. Rev.,* **108,** 92–96.

——, and M. Ek, 1993: Spatial variability of turbulent fluxes and roughness lengths in HAPEX-MOBILHY. *Bound.-Layer Meteor.,* **65,** 381–400.

Namias, J., 1988: The 1988 summer drought over the Great Plains—A classic example of air–sea–land interaction. *Trans. Amer. Geophys. Union,* **69,** 1067.

Nicholls, S., and C. J. Reading, 1979: Aircraft observations of the structure of the lower boundary layer over the sea. *Quart. J. Roy. Meteor. Soc.,* **105,** 785–802.

——, and M. A. LeMone, 1980: The fair-weather boundary layer in GATE: The relationship of subcloud fluxes and structure to the distribution and enhancement of cumulus clouds. *J. Atmos. Sci.,* **37,** 2051–2067.

Noilhan, J., and S. Planton, 1989: A simple parameterization of land surface processes for meteorological models. *Mon. Wea. Rev.,* **117,** 536–549.

Oglesby, R. J., and D. J. Erickson III, 1989: Soil moisture and the persistence of North American drought. *J. Climate,* **2,** 1362–1380.

Otterman, J., A. Manes, S. Rubin, P. Alpert, and D. O'C. Starr, 1990: An increase of early rains in southern Israel following land-use change? *Bound.-Layer Meteor.,* **53,** 333–351.

Palmén, E., and C. W. Newton, 1969: *Atmospheric Circulation Systems: Their Structure and Physical Interpretation.* Academic Press, 603 pp.

Pan, H.-L., and L. Mahrt, 1987: Interaction between soil hydrology and boundary layer development. *Bound.-Layer Meteor.,* **38,** 185–202.

Rabin, R. M., S. Stadler, P. J. Wetzel, D. J. Stensrud, and M. Gregory, 1990: Observed effects of landscape variability on convective clouds. *Bull. Amer. Meteor. Soc.,* **71,** 272–280.

Segal, M., G. Kallos, J. Brown, and M. Mandel, 1991: Morning temporal variations of shelter level specific humidity. *J. Appl. Meteor.,* **31,** 74–85.

Steyn, D. G., 1990: An advective mixed-layer model for heat and moisture incorporating an analytic expression for moisture entrainment. *Bound.-Layer Meteor.,* **53,** 21–31.

Stull, R. B., 1988: *An Introduction to Boundary Layer Meteorology.* Kluwer Academic Publishers, 666 pp.

Tennekes, H., 1973: A model for the dynamics of the inversion above a convective boundary layer. *J. Atmos. Sci.,* **30,** 558–567.

——, and A. G. M. Driedonks, 1981: Basic entrainment equations for the atmospheric boundary layer. *Bound.-Layer Meteor.,* **20,** 515–531.

Trenberth, K. E., G. W. Branstator, and P. A. Arkin, 1988: Origins of the 1988 North American drought. *Science,* **242,** 1640–1645.

Troen, I., and L. Mahrt, 1986: A simple model of the atmospheric boundary layer: Sensitivity to surface evaporation. *Bound.-Layer Meteor.,* **37,** 129–148.

Wilde, N. P., R. B. Stull, and E. W. Eloranta, 1985: The LCL zone and cumulus onset. *J. Climate Appl. Meteor.,* **24,** 640–657.